Emission location dependent ozone depletion potentials for very short-lived halogenated species

Ignacio Pisso, P. H. Haynes, Kathy S. Law

Atmos. Chem. Phys., 10, 12025–12036, 2010
www.atmos-chem-phys.net/10/12025/2010/
doi:10.5194/acp-10-12025-2010

Atmospheric Chemistry and Physics

Emission location dependent ozone depletion potentials for very short-lived halogenated species

I. Pisso[1,2,*], **P. H. Haynes**[1], **and K. S. Law**[2]

[1]DAMTP, University of Cambridge, Cambridge, UK
[2]UPMC Univ. Paris 06; Université Versailles St-Quentin en Yvelines; CNRS/INSU; LATMOS/IPSL, UMR 8190, Paris, France
[*]now at: Research Institute for Global Change, JAMSTEC, Yokohama, Japan

Received: 20 May 2010 – Published in Atmos. Chem. Phys. Discuss.: 30 June 2010
Revised: 16 November 2010 – Accepted: 20 November 2010 – Published: 17 December 2010

Abstract. We present trajectory-based estimates of Ozone Depletion Potentials (ODPs) for very short-lived halogenated source gases as a function of surface emission location. The ODPs are determined by the fraction of source gas and its degradation products which reach the stratosphere, depending primarily on tropospheric transport and chemistry, and the effect of the resulting reactive halogen in the stratosphere, which is determined by stratospheric transport and chemistry, in particular by stratospheric residence time. Reflecting the different timescales and physico-chemical processes in the troposphere and stratosphere, the estimates are based on calculation of separate ensembles of trajectories for the troposphere and stratosphere. A methodology is described by which information from the two ensembles can be combined to give the ODPs.

The ODP estimates for a species with a fixed 20 d lifetime, representing a compound like n-propyl bromide, are presented as an example. The estimated ODPs show strong geographical and seasonal variation, particularly within the tropics. The values of the ODPs are sensitive to the inclusion of a convective parametrization in the trajectory calculations, but the relative spatial and seasonal variation is not. The results imply that ODPs are largest for emissions from south and south-east Asia during Northern Hemisphere summer and from the western Pacific during Northern Hemisphere winter. Large ODPs are also estimated for emissions throughout the tropics with non-negligible values also extending into northern mid-latitudes, particularly in the summer. These first estimates, whilst made under some simplifying assumptions, show larger ODPs for certain emission regions, particularly south Asia in NH summer, than have typically been reported by previous studies which used emissions distributed evenly over land surfaces.

Correspondence to: I. Pisso
(ignacio@jamstec.go.jp)

1 Introduction

It is now well established that long-lived halocarbons (e.g. CFCs, HCFCs, solvents etc.) have contributed to the destruction of ozone in the stratosphere over at least the last 30 years (WMO, 2007). The impact of halogen containing substances on stratospheric ozone depletion has been quantified using Ozone Depletion Potentials (ODPs), which are defined as the time-integrated ozone depletion resulting from unit mass emission of that substance relative to that resulting from a corresponding unit mass emission of CFC-11 (CCl_3F) (Wuebbles, 1983; Solomon et al., 1992; WMO, 2007). ODPs are most easily defined for substances with long atmospheric lifetimes (greater than about 6 months). For these substances, which are well mixed in the troposphere, the ODP is independent of the emission time and location.

There is now increasing interest in stratospheric ozone depletion due to halogen-containing substances with lifetimes of 6 months or less, now conventionally called Very Short-lived Substances (VSLS). These are currently estimated to make a small contribution to the stratospheric chlorine loading (WMO, 2007) but a significant contribution to total stratospheric bromine, Br_y. This contribution has been inferred from stratospheric BrO data, independent estimates from upper tropospheric measurements of VSLS and modeling studies (e.g. Dorf et al., 2008; Kerkweg et al., 2008a,b; Aschmann et al., 2009; Hossaini et al., 2010) and is estimated to be 3 to 8 ppt bromine out of a total Br_y loading of 18 to

Published by Copernicus Publications on behalf of the European Geosciences Union.

25 ppt (WMO, 2007). Given that anthropogenic emissions of long-lived brominated halons and methyl bromide appear to be decreasing, the relative contribution of brominated VSLS to total stratospheric bromine, and hence to ozone depleting reactive bromine, is likely to increase in the future. Within the stratosphere reactive bromine destroys ozone more effectively, by a factor of 60, than reactive chlorine on an atom-by-atom basis (WMO, 2007). Reactive iodine species would destroy ozone even more effectively but are considered to be less important given current knowledge of emissions and hence of likely stratospheric iodine loading.

At the present time, VSLS emissions are dominated by natural emissions with only 5% or less coming from human sources although these may increase in the future. For example, n-propyl bromide, (nC_3H_7Br, hereafter n-PB) is a non-natural VSLS already used as a fumigant and proposed as a solvent replacement. Other VSLS have also been proposed such as iodotrifluoromethane (CF_3I) for use as a halon replacement and phosphoroustribromide (PBr_3) for in-flight aircraft engine fire suppression. Furthermore emissions of natural halogenated VSLS may increase as a result of climate change, e.g. from oceans in response to increasing sea surface temperatures (e.g. Butler et al., 2007).

VSLS are not well-mixed in the troposphere and therefore estimation of their ODPs needs to take into account the details of the spatial distribution of emissions. This point has been recognized for some time (Solomon and Albritton, 1992) but to date only a limited number of quantitative estimates exist (e.g. Wuebbles et al., 2001, 2009) since such estimates require the use of global models including both tropospheric and stratospheric processes. For each ODP assessment several model integrations are required at significant computational cost and due to large uncertainties in the spatial and temporal distributions of VSLS emissions, different emission scenarios also need to be evaluated.

A methodology is required which provides VSLS ODPs as a function of surface emission location directly. Here, we present such a methodology based on a trajectory modelling approach. The advantage of using trajectories is that transport characteristics from particular locations and their impact on ODPs can be clearly identified without the need to perform multiple integrations as in the case of ODP evaluation using global Eulerian models. The ODP depends on the fraction of VSLS, or more precisely the fraction of the total emitted halogen, emitted from a given location reaching the stratosphere and the residence time in the stratosphere, during which ozone depletion can occur due to the reactive halogen arising from the emission. Ensembles of tropospheric trajectories including a representation of total halogen degradation are used to quantify the fraction reaching the stratosphere. Stratospheric trajectories, run for longer time periods, are used to quantify stratospheric residence time. The information from the two sets of trajectories is combined to estimate the VSLS ODP as a function of emission location.

A major goal of this paper is to present the methodology (Sect. 2) and in this first step simplifying assumptions have been made with regard to VSLS processing, loss and impact on ozone. However, we believe that the conclusions are robust to relaxing these assumptions. ODPs are presented in Sect. 3 for a VSLS with a 20 d lifetime, representing a compound like n-PB, and compared to previous studies. Conclusions are given in Sect. 4.

2 Methodology

The processes controlling VSLS ODPs have been set out in WMO (2003, Chapter 2). As for long-lived species, any halogen-containing source gas (SG) emitted at the surface is exported into the free troposphere and thence potentially transported into the stratosphere. For VSLS in particular, a significant fraction of the SG is expected to degrade photochemically during the transit to the stratosphere, producing halogen-containing product gases (PG). The PG may themselves degrade photochemically, or since many are soluble, may be removed by rainout or by other cloud processes (WMO, 2007). The total halogen reaching the stratosphere potentially includes contributions from SG and PG.

Motivated by the above, the semi-empirical estimate for the ODP of a long-lived species was extended in WMO (2003) to a VSLS, X, to be:

$$\mathrm{ODP}_X(\mathbf{x}_\mathrm{e},t_\mathrm{e}) = (r_X^{\mathrm{SG}}(\mathbf{x}_\mathrm{e},t_\mathrm{e})\zeta_X^{\mathrm{SG}} + r_X^{\mathrm{PG}}(\mathbf{x}_\mathrm{e},t_\mathrm{e})\zeta_X^{\mathrm{PG}}) \cdot \frac{\alpha n_{\mathrm{Br}} + n_{\mathrm{Cl}}}{3} \cdot \frac{T_X^{\mathrm{active}}(\mathbf{x}_\mathrm{e},t_\mathrm{e})}{T_{\text{CFC-11}}^{\mathrm{active}}} \cdot \frac{M_{\text{CFC-11}}}{M_X} \quad (1)$$

where $\mathbf{x}_\mathrm{e}$ and t_e are, respectively the location and time of emission. This is essentially the form given in (2.14) of WMO (2003) presented in a notation that is more compatible with that for a long-lived species presented in WMO (2007). Here $r_X^{\mathrm{SG}}(\mathbf{x}_\mathrm{e},t_\mathrm{e})$ and $r_X^{\mathrm{PG}}(\mathbf{x}_\mathrm{e},t_\mathrm{e})$ respectively are the mass fractions of the source and product gases that reach the stratosphere (measured relative to the mass of the emitted source gas). $T_X^{\mathrm{active}}(\mathbf{x}_\mathrm{e},t_\mathrm{e})$ is the time spent in the stratosphere by the active halogen that results from the breakdown of X (and correspondingly for $T_{\text{CFC-11}}^{\mathrm{active}}$). Note that the possible dependence on $\mathbf{x}_\mathrm{e}$ and t_e is retained in $T_X^{\mathrm{active}}(\mathbf{x}_\mathrm{e},t_\mathrm{e})$. WMO (2003) refer to $T_X^{\mathrm{active}}(\mathbf{x}_\mathrm{e},t_\mathrm{e})$ as a stratospheric residence time, which can be justified on the basis that the active species that result from breakdown of X are soluble or have short tropospheric lifetimes, so that once the active species leaves the stratosphere and enters the troposphere it will be removed. n_{Br} and n_{Cl} are respectively the number of the bromine and chlorine atoms in one molecule of X and α is an "efficiency factor" for ozone destruction by reactive bromine relative to that by reactive chlorine. The efficiency factors ζ_X^{SG} and ζ_X^{PG} are included since the ozone depletion resulting from the halogen released by breakdown of source gases or product gases will not depend only on the residence time

$T_X^{\text{active}}(\mathbf{x}_e, t_e)$ but also on details of where exactly the halogen is released and on its subsequent path through the stratosphere. For the remainder of this paper ζ_X^{SG} and ζ_X^{PG} are both taken to be equal to 1 (but they could be estimated more precisely from a suitable model calculation). These factors should also arguably depend on $\mathbf{x}_e$ and t_e but this dependence has been ignored as a first approximation. Mass fractions are converted into molar fractions by the quotient $\frac{M_{\text{CFC}-11}}{M_X}$ of molecular masses of CFC−11 and X. Note that the Eq. (1) holds not only for VSLS, but also for a long-lived species, for which $r^{\text{SG}} = 1$ and $r^{\text{PG}} = 0$. The Eq. (1) highlights that in estimating ODPs for VSLS there are two major and somewhat independent considerations. The first is the path taken through the troposphere, which determines $r_X^{\text{SG}}(\mathbf{x}_e, t_e)$ and $r_X^{\text{PG}}(\mathbf{x}_e, t_e)$, and the second is the path taken through the stratosphere, which determines $T_X^{\text{active}}(\mathbf{x}_e, t_e)$. Given knowledge of $\text{ODP}_X(\mathbf{x}_e, t_e)$, the ODP for an arbitrary emission distribution in location and time can be calculated by a weighted integral of $\text{ODP}_X(\mathbf{x}_e, t_e)$.

The processes removing SG and PG are distinct, and for detailed calculations of ozone depletion the partitioning of halogen reaching the stratosphere between SG and PG may be important (WMO, 2007). However, in a first-order description, what is important is the total halogen reaching the stratosphere. In the following development of a method for calculating ODPs for VSLS we shall, for simplicity, assume that it is sufficient to consider total halogen, i.e. to regard X as a family that includes the SG and all the resulting halogen-containing PG and degradation products, but it would be straightforward to extend the method and relax this assumption.

Consider now the depletion of ozone in the stratosphere, recalling that ODPs are fundamentally a linear concept that quantifies the effect of a unit emission on a given background atmosphere. Therefore, during its passage across the stratosphere, X can be taken to destroy ozone, measured by mass concentration, at a local rate which is proportional to the local mass concentration of X, with a constant of proportionality equal to K_X, so that K_X has units of inverse time. K_X encodes information not only on the reactivity, but also on the fraction of X (recall that X is now being regarded as a chemical family) that appears in active form together with the background concentrations of ozone and other species that influence the rate of destruction.

The time integrated depletion of ozone in a region Ω of the stratosphere due to a unit mass emission of X released at location $\mathbf{x}_e$ and time t_e in the troposphere can therefore be written as:

$$\Delta\text{O}_3(X, \mathbf{x}_e, t_e) = \int_{t_e}^{\infty} \int_{\Omega} \rho_X(\mathbf{x}, t, \mathbf{x}_e, t_e) K_X(\mathbf{x}, t) d\mathbf{x} dt \qquad (2)$$

The integration variables $\mathbf{x}$ and t represent positions and times in the stratosphere. $\rho_X(\mathbf{x}, t, \mathbf{x}_e, t_e)$ is the density of X (total halogen) at position $\mathbf{x}$ and time t resulting from the pulse emission of X at position $\mathbf{x}_e$ and time t_e.

Evaluation of the integral in Eq. (2) requires prediction of the density $\rho_X(\mathbf{x}, t, \mathbf{x}_e, t_e)$ through solution of the equations for transport and chemical reaction given the pulse emission at $\mathbf{x}_e, t_e$. This prediction could be based on an Eulerian chemical transport model, but here we follow chemical evolution along trajectories using a Lagrangian approach. In other words we assume that:

$$\rho_X(\mathbf{x}, t, \mathbf{x}_e, t_e) = \langle r_X(t; \mathbf{X}) \delta(\mathbf{x} - \mathbf{X}(t; \mathbf{x}_e, t_e)) \rangle \qquad (3)$$

where $\mathbf{x}$=$\mathbf{X}(t; \mathbf{x}_e, t_e)$ describes, as t varies, a trajectory beginning at position $\mathbf{x}_e$ at time t_e. $\delta()$ is the Dirac delta function. $r_X(t; \mathbf{X})$ is a number between 0 and 1 representing the variation of total amount of halogen species X, so that $r_X(t_e; \mathbf{x}_e) = 1$, with $r_X(t; \mathbf{X}(t; \mathbf{x}_e, t_e))$ expected to decay as t increases from t_e. The brackets $\langle\rangle$ denote an average over a suitable ensemble of trajectories emitted at $\mathbf{x}_e, t_e$ carrying initially a unit mass of the species X in SG form. This averaging could, for example, reflect the fact that variation of $\Delta\text{O}_3(X, \mathbf{x}_e, t_e)$ with respect to $\mathbf{x}_e$ or t_e is necessarily coarse-grained – i.e. an ensemble of trajectories with launch position close to $\mathbf{x}_e$ or launch time close to t_e is considered and an average is taken over that ensemble, or it could be that some kind of stochastic parametrization is required in following the trajectory $\mathbf{X}(t; \mathbf{x}_e, t_e)$, e.g. many realisations of a random walk representing diffusion (e.g. Legras et al., 2003) or indeed convective effects, followed by an average over an ensemble of such realisations.

We may substitute Eq. (3) into Eq. (2), to give

$$\begin{aligned} &\Delta\text{O}_3(X, \mathbf{x}_e, t_e) \\ &= \langle \int_{t_e}^{\infty} dt \int_{\Omega} d\mathbf{x}\, r_X(t; \mathbf{X}) \delta(\mathbf{x} - \mathbf{X}(t; \mathbf{x}_e, t_e)) K_X(\mathbf{x}, t) \rangle \\ &= \langle \int_{t_{\text{in}}(\Omega, \mathbf{X})}^{\infty} dt\, r_X(t; \mathbf{X}) K_X(\mathbf{X}(t; \mathbf{x}_e, t_e), t) \rangle \end{aligned} \qquad (4)$$

where $t_{\text{in}}(\Omega, \mathbf{X})$ is the time at which the trajectory $\mathbf{X}$ first enters the stratosphere. $t_{\text{out}}(\Omega, \mathbf{X})$ may be defined correspondingly as the time the trajectory first leaves the stratosphere.

Note that if followed long enough the trajectory $\mathbf{X}$ will enter and leave the stratosphere many times. However the active part of the halogen will, to good approximation, leave only once since, once it re-enters the troposphere it will be rapidly lost due to rainout.

We can instead write $K_X = \chi_X^{\text{active}} K_X^{\text{active}}$ where χ_X^{active} is the proportion of X appearing in the active form and then regard χ_X^{active} not as representing the active part of X arising in a single circuit of the trajectory through the stratosphere, but as a sum of the parts arising in all such circuits. The active fraction χ_X^{active} corresponds to the factors ζ^{SG} and ζ^{PG} in Eq. (1). The integral appearing in Eq. (4) is then not taken over the entire trajectory subsequent to first entry into the stratosphere, but instead only over the part of the trajectory corresponding to first passage through the stratosphere, i.e. the upper limit of the integral is taken to be $t_{\text{out}}(\Omega, \mathbf{X})$ rather than ∞. Note that the need to consider the sum over

all circuits applies only to a long-lived species, since it might reasonably be assumed that for VSLS the conversion to the active form during one circuit is complete, but the generalisation is useful since the resulting formalism then applies to all halogenated substances, regardless of lifetime.

This alternative formulation allows $r_X(t;\mathbf{X})$ to be considered constant for $t>t_{\rm in}(\Omega,\mathbf{X})$. The subsequent loss of total halogen is incorporated by the definition of $\chi_X^{\rm active}$ as the cumulative distribution function for conversion to the active species, regarded as function of position and then sampled by the trajectory. The change of the upper limit to the integral allows Eq. (4) to be re-expressed as:

$$\Delta {\rm O}_3(X,\mathbf{x}_{\rm e},t_{\rm e})=\langle r_X(t_{\rm in}(\Omega);\mathbf{X})\int_{t_{\rm in}(\Omega,\mathbf{X})}^{t_{\rm out}(\Omega,\mathbf{X})} dt\,\chi_X^{\rm active}(\mathbf{X}(t;\mathbf{x}_{\rm e},t_{\rm e}))K_X^{\rm active}(\mathbf{X}(t;\mathbf{x}_{\rm e},t_{\rm e}))\rangle \quad (5)$$

where the factor $r_X(t_{\rm in}(\Omega),\mathbf{X})$ in Eq. (5) is determined by the tropospheric trajectory segments and the integral is determined by the stratospheric trajectories. For VSLS, $r_X(t_{\rm in}(\Omega),\mathbf{X})$ is expected to be significantly less than one, since total halogen, in both SG and PG, reaching the stratosphere is expected to be only a small fraction of that emitted. For long-lived species, on the other hand, we expect $r_X(t_{\rm in}(\Omega),\mathbf{X})=1$. Note that the integral in Eq. (5), whilst evaluated only over the stratospheric portion of each trajectory, depends implicitly on the tropospheric portion through $\mathbf{x}_{\rm e}$ and $t_{\rm e}$. We make the further important simplification that this dependence is only through the entry point $\mathbf{X}_{\rm in}=\mathbf{X}(t_{\rm in};\mathbf{x}_{\rm e},t_{\rm e})$ and entry time $t_{\rm in}$, i.e. the final point on the first tropospheric portion of the trajectory and the initial point on the subsequent stratospheric portion.

This allows the above expression for $\Delta {\rm O}_3(X,\mathbf{x}_{\rm e},t_{\rm e})$ to be rewritten as:

$$\begin{aligned}&\Delta {\rm O}_3(X,\mathbf{x}_{\rm e},t_{\rm e})\\&=\int_{t_{\rm e}}^{\infty}ds\int_{\partial\Omega}d\mathbf{y}\sigma(\mathbf{y},s;\mathbf{x}_{\rm e},t_{\rm e})\langle r_X(t_{\rm in}(\Omega);\mathbf{X})|\mathbf{X}_{\rm in}=\mathbf{y},t_{\rm in}=s\rangle\\&\times\langle\int_{t_{\rm in}(\Omega,\mathbf{X})}^{t_{\rm out}(\Omega,\mathbf{X})}dt\,\chi_X^{\rm active}(\mathbf{X}(t;\mathbf{x}_{\rm e},t_{\rm e}))K_X^{\rm active}(\mathbf{X}(t;\mathbf{x}_{\rm e},t_{\rm e}))|\mathbf{X}_{\rm in}=\mathbf{y},t_{\rm in}=s\rangle\\&=\int_{t_{\rm e}}^{\infty}ds\int_{\partial\Omega}d\mathbf{y}\sigma(\mathbf{y},s;\mathbf{x}_{\rm e},t_{\rm e})r_X^{\Omega}(\mathbf{y},s,\mathbf{x}_{\rm e},t_{\rm e})\bar{K}_X^{\rm active}T_X^{\rm active}(\mathbf{y},s)\end{aligned} \quad (6)$$

where $\partial\Omega$ is the surface bounding the region Ω (across which all trajectories entering Ω must pass), $\sigma(\mathbf{y},s)$ is the probability density function for entry location $\mathbf{y}$ and entry time s, $r_X^{\Omega}(\mathbf{y},s,\mathbf{x}_{\rm e},t_{\rm e})=\langle r_X(t_{\rm in}(\Omega);\mathbf{X})|\mathbf{X}_{\rm in}=\mathbf{y},t_{\rm in}=s\rangle$ and $\bar{K}_X^{\rm active}T_X^{\rm active}(\mathbf{y},s)=\langle\int_{t_{\rm in}(\Omega,\mathbf{X})}^{t_{\rm out}(\Omega,\mathbf{X})}dt\,\chi_X^{\rm active}K_X^{\rm active}(\mathbf{X}(t;\mathbf{x}_{\rm e},t_{\rm e}))|\mathbf{X}_{\rm in}=\mathbf{y},t_{\rm in}=s\rangle$, with the constant $\bar{K}_X^{\rm active}$ some suitable average of $K_X^{\rm active}(\mathbf{X})$. The notation $\langle .|\mathbf{X}_{\rm in}=\mathbf{y},t_{\rm in}=s\rangle$ is used to denote an average over all trajectories with entry point $\mathbf{y}$ and entry time s.

Note the correspondence between the factors appearing in Eq. (6) and those appearing in Eq. (1). $r_X^{\Omega}(\mathbf{y},s,\mathbf{x}_{\rm e},t_{\rm e})$ corresponds to a combination of $r_X^{\rm SG}$ and $r_X^{\rm PG}$, i.e. the proportion of total halogen that reaches the stratosphere (in both source and product form), and

$$T_X^{\rm active}(\mathbf{y},s)=\langle\int_{t_{\rm in}(\Omega,\mathbf{X})}^{t_{\rm out}(\Omega,\mathbf{X})}dt\,\chi_X^{\rm active}|\mathbf{X}_{\rm in}=\mathbf{y},t_{\rm in}=s\rangle$$

corresponds to $T_X^{\rm active}$, i.e. the stratospheric residence time for active halogen, but these are for given location $\mathbf{x}_{\rm e}$ and time $t_{\rm e}$ of release (only for the factor $r_X^{\Omega}(\mathbf{y},s,\mathbf{x}_{\rm e},t_{\rm e})$) and given entry location $\mathbf{y}$ and entry time s into the stratosphere (for both factors $r_X^{\Omega}(\mathbf{y},s,\mathbf{x}_{\rm e},t_{\rm e})$ and $T_X^{\rm active}(\mathbf{y},s)$). Note in particular that we have chosen to retain the possibility of dependence of stratospheric residence time on stratospheric entry location and time.

The Eq. (6) is calculated in practice using two ensembles of forward trajectories. The first is a tropospheric ensemble, used to evaluate $\sigma(\mathbf{y},s;\mathbf{x}_{\rm e},t_{\rm e})r_X^{\Omega}(\mathbf{y},s,\mathbf{x}_{\rm e},t_{\rm e})$. A second, stratospheric, trajectory ensemble is used to evaluate $T_X^{\rm active}(\mathbf{y},s)$. The division of the calculation in this way has two advantages that, first, differences in transport time scales between troposphere and stratosphere are taken into account and, second, differences between tropospheric and stratospheric chemical processes can be exploited. Consider first the tropospheric part of the calculation.

Trajectories are integrated forward in time from a space-time (emission) grid at the Earth's surface for $\mathbf{x}_{\rm e}$ and $t_{\rm e}$. A corresponding space-time grid for $\mathbf{y}$ and s is specified on the control surface $\partial\Omega$ defining the boundary of the stratosphere. The trajectory calculation then gives, for example, the fraction of the trajectories released from a space-time grid-box at the Earth's surface which reach a particular space-time grid box on the control surface $\partial\Omega$. Given some procedure for calculating the proportion of total halogen $r_X^{\Omega}(\mathbf{y},s,\mathbf{x}_{\rm e},t_{\rm e})$ which reaches the stratosphere via this route, with the simplest possible procedure being to assume exponential decay at rate λ, this allows estimation of the product $\sigma(\mathbf{y},s;\mathbf{x}_{\rm e},t_{\rm e})r_X^{\Omega}(\mathbf{y},s,\mathbf{x}_{\rm e},t_{\rm e})$ appearing in Eq. (6). In the following section we will take $\lambda^{-1}=20$ d corresponding to an n-PB-like substance.

Now consider the stratospheric part of the calculation. For this trajectories are integrated forward in time from the control surface $\partial\Omega$ with its space-time grid specifying the variables $\mathbf{y}$ and s. If X is a VSLS then we make the simplest possible assumption that $\chi_X^{\rm active}=1$ everywhere in the stratosphere, i.e. that on entering the stratosphere all SG and PG are converted to active form. The results presented by Hossaini et al. (2010), particularly the profiles shown in their Fig. 11, for $CHBr_3$ (which is believed to have a tropospheric lifetime of around 25 d), provide some justification for this. It follows that $T_X^{\rm active}(\mathbf{y},s)$ is then precisely the stratospheric residence time $T_{\rm res}^{\rm strat}(\mathbf{y},s)$ say, for trajectories entering the stratosphere at position $\mathbf{y}$ and time s and the required estimate

of this function is simply the average time for trajectories leaving the appropriate grid box on the control surface Ω to re-enter the troposphere. This procedure is likely to be incorrect for $T^{\text{active}}_{\text{CFC-11}}$ however, since the source region for the active products of CFC-11 is not close to the tropopause. Therefore we simply set $T^{\text{active}}_{\text{CFC-11}}$ to be a constant value equal to the stratospheric residence time from a starting point in the tropical middle stratosphere, corresponding to an assumption that the production of active chlorine from the partial breakdown of the CFC-11 occurs only at this point.

Combining the estimates of $\sigma(\mathbf{y},s;\mathbf{x}_\text{e},t_\text{e})r^{\Omega}_X(\mathbf{y},s,\mathbf{x}_\text{e},t_\text{e})$ from the tropospheric trajectory calculation and of $T^{\text{strat}}_{\text{res}}(\mathbf{y},s)$ from the stratospheric trajectory calculation and summing over grid boxes corresponding to $\mathbf{y}$ and s gives the required estimate for $\Delta O_3(X,\mathbf{x}_\text{e},t_\text{e})$. On the other hand $\Delta O_3(\text{CFC-11})=\bar{K}^{\text{active}}_{\text{CFC-11}}T^{\text{active}}_{\text{CFC-11}}$, is independent of location and time of emission. For a brominated VSLS, recalling Eq. (1) and that the ratio $\bar{K}^{\text{active}}_X/\bar{K}^{\text{active}}_{\text{CFC-11}}$ is equal to $(\alpha n_{\text{Br}}+n_{\text{Cl}})/3$, it follows from Eq. (6) that:

$$\text{ODP}_X(\mathbf{x}_\text{e},t_\text{e}) = \frac{M_{\text{CFC-11}}}{M_X}\frac{\alpha n_{\text{Br}}+n_{\text{Cl}}}{3T^{\text{active}}_{\text{CFC-11}}}\int_{t_\text{e}}^{\infty} ds \int_{\partial\Omega} d\mathbf{y}\sigma(\mathbf{y},s;\mathbf{x}_\text{e},t_\text{e})r^{\Omega}_X(\mathbf{y},s,\mathbf{x}_\text{e},t_\text{e})T^{\text{strat}}_{\text{res}}(\mathbf{y},s) \quad (7)$$

3 Results and discussion

The methodology described in the previous section requires separate tropospheric and stratospheric trajectory calculations. Velocity fields from the ERA Interim reanalysis dataset were used to calculate trajectories with FLEXPART (Stohl et al., 2005). Two versions of the tropospheric calculations were carried out, one simply using the reanalysis velocity fields and the other including the Emanuel parametrization of deep convection implemented in FLEXPART as reported by Stohl et al. (2005) and Forster et al. (2007). The tropospheric forward trajectories were started in January and July 2001 from points distributed over a 1 degree latitude-longitude grid and over 19 levels in the boundary layer every 50 m up to 950 m giving 1.2 million trajectories for each starting time. The trajectories were followed for 12 months and positions recorded every 12 h. The combined effects of SG oxidation by OH and PG rainout were represented in a very simple way by assuming that the total amount of halogen associated with the VSLS, X, decayed exponentially at a rate λ, with $\lambda^{-1}=20$ d corresponding to a nPB-like VSLS (Wuebbles et al., 2009).

The lower boundary for the stratosphere volume, Ω, was taken to be the 380 K surface. The fraction of total halogen crossing this surface as a function of emission location:

$$\int_{t_\text{e}}^{\infty} ds \int_{\partial\Omega} d\mathbf{y}\sigma(\mathbf{y},s;\mathbf{x}_\text{e},t_\text{e})r^{\Omega}_X(\mathbf{y},s,\mathbf{x}_\text{e},t_\text{e}) \quad (8)$$

extracted from Eq. (6), is shown in Fig. 1 for January and July for runs with and without convection. The results show that the injected fraction is always greater when convection is included although runs with and without convection show similar latitude and longitude variations in the tropics where the fraction is largest.

The spatial variation of the emitted species fraction transported to the stratosphere (Fig. 1) shows a dominant source region for air reaching the tropical tropopause region over the equatorial west Pacific region in Northern Hemisphere (NH) winter which moves northward and extends westwards to include south-east and south Asia in NH summer. This is broadly as expected from previous trajectory studies (Fueglistaler et al., 2004; Berthet et al., 2007) and (for NH winter only) the Eulerian study of Aschmann et al. (2009). The localisation of the source regions for rapid transport to the stratosphere is consistent with current ideas that only outflow from only the highest convection is likely to ascend into the stratosphere on short time scales (e.g. Fueglistaler et al., 2009, and references therein). Note that the study by Levine et al. (2007) shows less localisation, but they consider transport into the stratosphere not only via the tropical tropopause, but also quasi horizontally into the lowermost stratosphere.

To estimate VSLS ODPs, the fraction of halogen injected across the 380 K surface at location $\mathbf{y}$ and time s needs to be weighted by the stratospheric residence time $T^{\text{strat}}_{\text{res}}(\mathbf{y},s)$. This is estimated for every month with an ensemble (2.2 million) of stratospheric trajectories, on a $2^\circ\times2^\circ$ grid, using a seasonally varying, but perpetual year 2000, wind fields from ERA-Interim. In order to diagnose the time spent during the first passage through the stratosphere the trajectories were followed for 20 yr, significantly longer than standard estimates of lower stratospheric turnover time. The trajectories were judged to have left the stratosphere when they first crossed the WMO thermal tropopause also deduced from ERA-Interim data. Figure 2 displays $T^{\text{strat}}_{\text{res}}(\mathbf{y},s)$ for trajectories leaving the 380 K surface as a function of starting latitude and month. The results show a clear seasonal cycle, with, in the tropics, significant variability in the residence times. $T^{\text{strat}}_{\text{res}}(\mathbf{y},s)$ is shown in Fig. 3 as function of potential temperature and latitude calculated using ensembles of trajectories starting on several different potential temperature surfaces. It exhibits a pattern that might be expected from the large-scale stratospheric circulation and indeed $T^{\text{strat}}_{\text{res}}(\mathbf{y},s)$ is complementary to stratospheric age of air, which is a more standard and familiar diagnostic of the circulation (e.g. Waugh and Hall, 2002). For example, the effect of the tropical pipe can be seen at the Equator above 500 K, with a clear maximum in residence time due to that fact that an air parcel starting at this location will be taken upwards in the tropical pipe before then descending in the extratropics. As discussed in the previous section, the results displayed in Figs. 2 and 3 can be used to estimate a residence time for reactive halogen produced by CFC-11 of about 60 months assuming that it breaks down in the tropical stratosphere above 20 km ($\simeq$530 K).

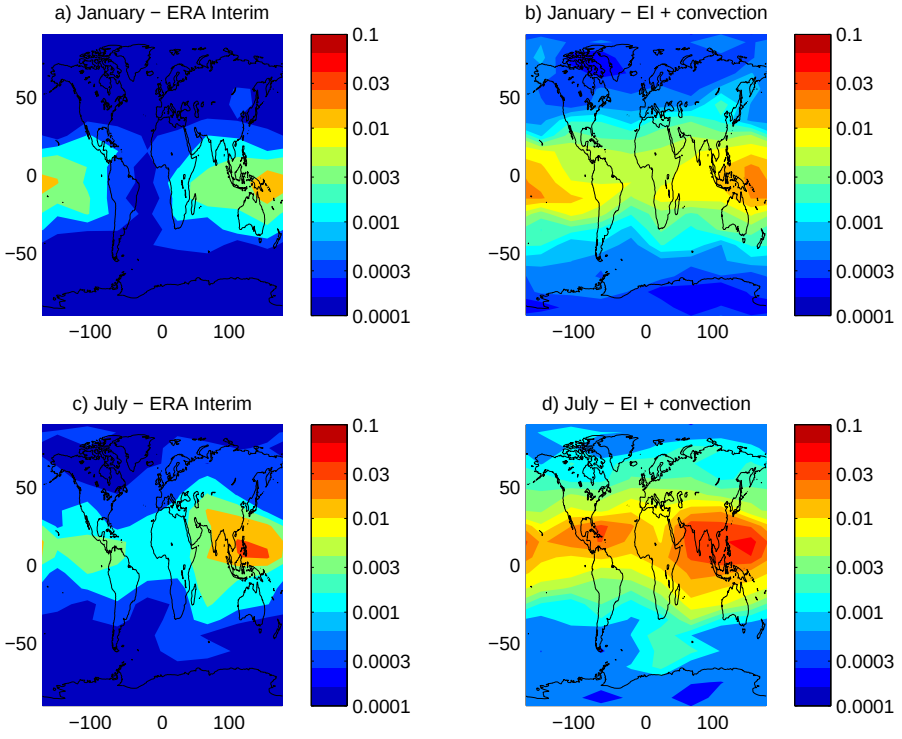

Fig. 1. Fraction of accumulated halogen reaching the 380 K surface within one year of a pulse emission of an nPB-like substance shown as a function of surface location of the emission. The fraction is estimated using forward trajectories started near the surface. **(a)** and **(b)** correspond to January 2001. **(c)** and **(d)** correspond to July 2001. **(a)** and **(c)** use ERA Interim vertical velocities. **(a)** and **(c)** use ERA Interim with the Emanuel convective parametrization as implemented in FLEXPART 6.2. See text for details.

Based on the results from the tropospheric and stratospheric trajectory calculations, ODPs can be calculated from Eq. (7). Again for illustrative purposes, and consistent with the assumed 20 d lifetime, we consider a VSLS like n-PB as an example with $n_{\mathrm{Br}} = 1$, $n_{\mathrm{Cl}} = 0$, $n_{\mathrm{Cl}}(\text{CFC-11}) = 3$, $T^{\mathrm{active}}_{\text{CFC-11}} = 60$ months, $M_{\text{CFC-11}}/M_X = 137.37/123.0 \simeq 1$ and $\alpha = 60$. Figure 4 shows the resulting ODP distribution for January and July 2000 as a function of surface emission location, for calculations without and with the convective parametrisation. Including the convective parametrisation enhances ODPs by up to a factor of 2. For example, with the convective parametrisation, ODPs in NH summer exceed 0.6 for emissions over southern Asia and have values of up to 0.2 for emissions over Central America. Maximum values are not significantly changed without the convective parametrisation, but values over the tropics as a whole are somewhat reduced. There is at least a factor of 4 reduction in the longitudinal average in the tropics compared to the extratropics. With the convective parametrisation, summer ODPs of around 0.03 are found for emissions at northern mid-latitudes, e.g. northern Europe, with values in excess of 0.1 for emissions at latitudes corresponding to southern Europe and the northern United States (US). These extratropical values are typically reduced by a factor of 3 or so in runs without the convective parametrization. It is worth noting that legislation in the US sets a limit of 0.2 for substances which are not controlled and the US Environmental Protection Agency cautions that chemicals with ODPs greater than 0.05 should be considered carefully (Wuebbles et al., 2009).

The ODP spatial distribution is similar to that of the quantity shown in Fig. 1 in terms of where the maxima are located. This similarity suggests that the effect of spatial variation in the stratospheric residence time is relatively weak. However, it is important to realise that the similarity in spatial distribution results primarily from the concentration in the tropics and, in particular, this means that it is the stratospheric residence time associated with tropical injection that determines the ODP. Using a global average value (over injection locations) of the stratospheric residence time would underestimate the ODP by a factor of 2 or so.

As noted for the fraction injected into the stratosphere (Fig. 1) the ODP results also show strong longitudinal variation (factor 3 or more) within the tropics as well as a strong seasonal variations. They suggest that ODPs for emissions from southern Asia in NH summer may be larger than for emissions from the western Pacific in NH winter. In NH summer significant ODP values extend southwards over the Indian ocean well beyond what are generally regarded as

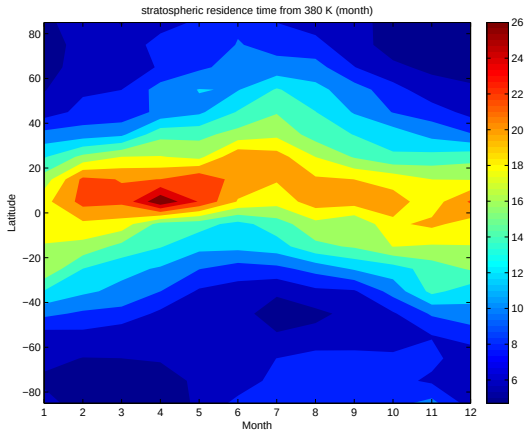

Fig. 2. Zonally averaged stratosphere residence time (see text) (colour indicates months) for airmasses starting on the 380 K surface as a function of latitude and time of the year of the starting point. Trajectories were integrated using perpetual year 2000 velocity fields from the ERA Interim dataset. See text for details.

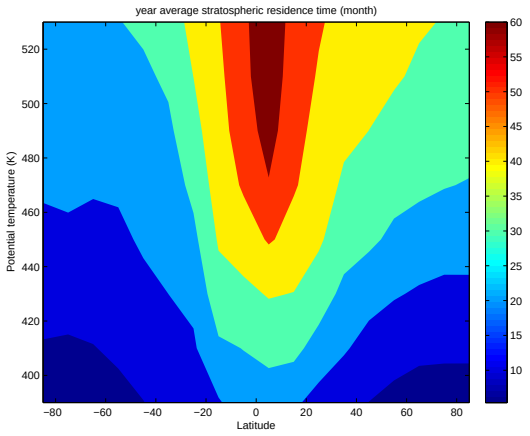

Fig. 3. Latitude-height cross section of stratospheric residence time for trajectories starting at different heights, from 380 K to 540 K, and latitudes. Trajectories were integrated using perpetual year 2000 velocity fields from the ERA Interim dataset. See text for details.

regions of active convection. This is consistent with the expected northward cross-equatorial flow into the convective regions and emphasises that the spatial distribution of ODPs is determined not only by the location of the most active convective regions but also by the pattern of low-level flow into those regions. Note that for the calculation without convection, the maximum ODPs over Asia are not reduced much relative to the calculations with convection but extend over a smaller region. A secondary maxima can also be seen over central America in NH summer.

WMO (2007) (Sect. 2.6.2) give an order of magnitude estimate for the ODP of a VSLS, such as n-PB, containing one bromine atom and with a molecular weight similar to CFC-11. They estimated that the fraction reaching stratosphere might typically range between 10^{-3} and 10^{-2} for a species with a lifetime of 25 d, according to emission location. Our calculations indicate that this fraction might be as much as 10^{-1} in certain regions (see Fig. 1), and that ODPs might be as large as 0.6 in these regions, as indicated in Fig. 4. Global mean ODPs for the 20 d tracer shown here vary from 0.021 and 0.035 in January and July in runs without convection to 0.067 and 0.079 in runs with convection. Results for different latitude bands for January and July for runs with and without convection are shown in Table 1.

These estimates are generally higher than previous estimates for n-PB based on emissions located in northern mid-latitudes (WMO, 2003, 2007). Wuebbles et al. (2001) estimated n-PB ODPs ranging from 0.033 to 0.040 for emissions over land and 0.021 to 0.028 for emissions over industrialized regions in the Northern Hemisphere. More recently, Wuebbles et al. (2009) re-evaluated n-PB OPDs finding values in mid-latitudes of 0.019 based on 2-D model calculations and 0.005 based on a 3-D model. These results, which

Table 1. Estimated ODPs for the nPB-like substance as a function of emission location, area-averaged over different latitude bands.

	Jan_{noconv}	Jan_{conv}	Jul_{noconv}	Jul_{conv}
60° N–90° N	0.0041	0.0143	0.0081	0.0217
30° N–60° N	0.0052	0.0266	0.0289	0.0654
30° S–30° N	0.1321	0.3027	0.1736	0.3285
30° S–60° S	0.0108	0.0333	0.0091	0.0213
60° S–90° S	0.0016	0.0114	0.0043	0.0138

are annual means over land surfaces where the substances were emitted, are lower than the results presented in Table 1, especially when convection is taken into account. However, the global model estimates included convection and also a rather detailed treatment of n-PB degradation. They included new kinetic data for the degration of an important n-PB product gas, bromoacetone (BrAc) finding a shorter lifetime (around 5 h) compared to previous studies. They estimated a lifetime for n-PB of around 24 d using both the 2-D and 3-D models. Wuebbles et al. (2009) also found a factor of 2 difference between mid-latitude (30°–60° N) and tropical (20° S–20° N) regions for another VSLS, CF_3I. Our estimates suggest a much larger difference (factor 5 to 11 in the runs with convection) between tropical and extratropical values. Recently, Wuebbles et al. (2010) have refined these values of ODP for nPB in the band 30° N–60° N to 0.0049 and the lifetime to 24.7 days and in the 60° S–70° N band a mean of 0.011 with a lifetime of 19.6 days.

The estimates of ODPs shown in Fig. 4 are, of course, dependent on the assumptions underlying the modelling methodology outlined in Sect. 2 and, in particular use of a trajectory-based approach. There is reason to believe that

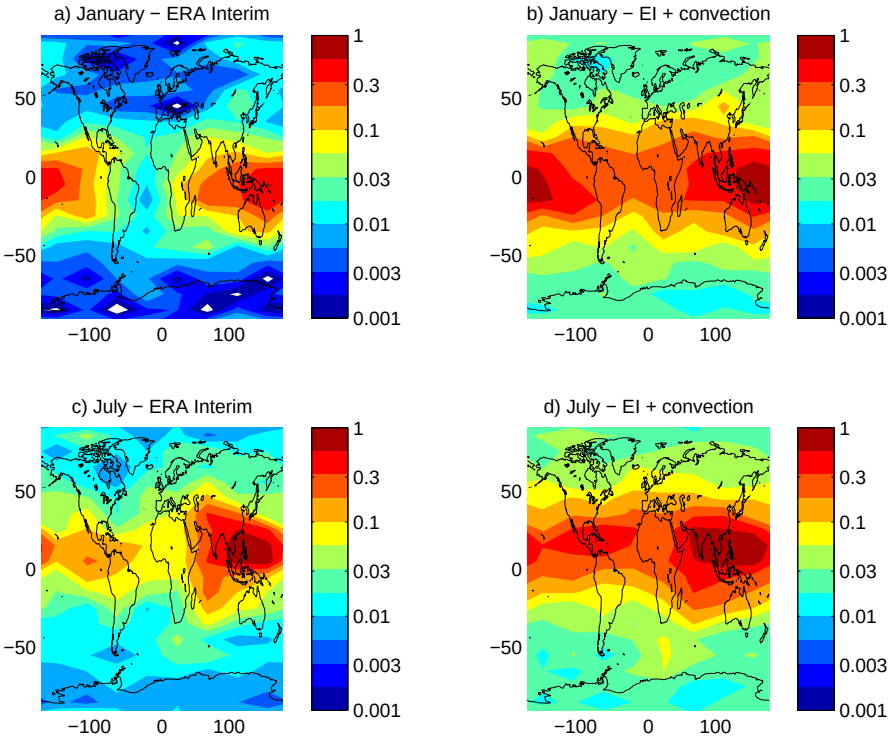

Fig. 4. Ozone Depletion Potentials for the nPB-like (20 d lifetime) substance as a function of latitude and longitude of emission location. **(a)** and **(b)** correspond to January 2001. **(c)** and **(d)** correspond to July 2001. **(a)** and **(c)** use ERA Interim vertical velocities. **(a)** and **(c)** use ERA Interim with the Emanuel convective parametrization as implemented in FLEXPART 6.2.

trajectories based on large-scale wind fields alone underestimate rapid vertical transport in the tropics. For example, Law et al. (2010) have suggested that use of such trajectories underestimates the contribution of deep convection over Asia to the air masses in the tropical tropopause layer (TTL) observed over west Africa and estimates of convective transport based on trajectories calculated explicitly in a mesoscale model appear to show deeper transport of air masses into the tropical tropopause layer (Fierli et al., 2010). The inclusion of the convective parameterization in the FLEXPART trajectory code clearly has a significant impact on our results and may go some way to improving the representation of transport based on large-scale trajectories alone. Nevertheless, large uncertainties remain and it would be interesting to repeat the present experiment with different convective parametrisations. Wuebbles et al. (2010) used MOZART driven by CCM3 winds. Moist convection in the CCM3 includes the deep convection scheme developed by Zhang and McFarlane (1995) which operates in conjunction with the scheme of Hack (1994). Tost et al. (2010) compared different convective parametrisation schemes in a global CTM, showing that the choice of the convection parametrisation in a global model of the chemical composition of the atmosphere has a substantial influence on trace gas distributions. In Fig. 2 of Tost et al. (2010), it is apparent that Emanuel parametrisation injects more mass across the 250 mb surface in the tropics than the scheme of Zhang and McFarlane. For example panel b shows differences of the order of 100% for ^{222}Rn between Zhang and McFarlane and Emanuel above 200 mb.

Increased injected mass across the 380 K surface in the tropics may be among the causes for the larger ODP estimates in the tropics here relative to Wuebbles et al. (2009, 2010) in addition to uncertainties related to the treatment of both tropospheric and stratospheric chemistry. It is worth remarking that the divergences appear mainly within the tropical belt and with the Emanuel parametrisation since our values for midlatitudes driven with ERA Interim winds and those in Wuebbles et al. (2009, 2010) are of a comparable order of magnitude. The assumptions related to stratospheric chemistry also introduce limitations for the accurate calculation of ODPs and may also explain some of the differences between our estimates and other numbers found in the literature. Another possible cause is an underestimation of the total ozone destroyed by CFC-11. In fact, CFC effect in the stratosphere is estimated using a full description of the stratospheric turnover of the injected masses yielding an expected residence time depending on the latitude and height, rather than a simple global mean residence time. CFC-11 is modelled as being activated above 30 hPa, but at this height the expected residence estimated is rather a lower boundary since we have used a 20 year trajectory calculation and at this height trajectories may remain in the stratosphere

for longer periods. A full assessment of the stratospheric expected residence time and age of stratospheric air would be advisable to address such an uncertainty. Eulerian model studies such as Wuebbles et al. (2009, 2010) may not have made such approximations of the stratospheric chemistry. In the real stratosphere, the amount of ozone destroyed by chlorine/bromine will not just depend linearly on the time spent in the stratosphere. If an air parcel reaches a high altitude, where the photochemical lifetime of ozone is short then ozone will reach equilibrium. In addition, bromine chemistry is not so efficient at these altitudes (WMO, 2007; Salawitch et al., 2005). In our approach, the different activation heights of chlorine from CFC-11 (above 30 hPa) and bromine from VSLS (above 380 K) aims to represent the inhomogeneous distribution of active species and other factors influencing the depletion reactions. The chlorine from CFC-11 and bromine from VSLS released is then modelled as remaining active along the transit through the stratosphere until the parcel under consideration is expelled back into the troposphere. This approximation largely neglects effects arising from the inhomogeneous distribution of active (radical) and inactive (reservoir) halogen; instead, only a mean efficiency factor α published in the literature (WMO, 2003, 2007) was assumed. This assumption could be relaxed in future studies but would add significant computational costs from running box models along the stratospheric trajectories.

The prediction of higher fractions of VSLS emissions reaching the stratosphere in NH summer, in particular, from southern Asia, than in NH winter, and the correspondingly higher ODPs for tropical emissions in NH summer versus those in NH winter is interesting. There are hints of this in previous results, e.g. results from the 1-D model study of Gettelman et al. (2009) show CO values that are larger in the lower stratosphere for NH summer over southern Asia than for NH winter over the west Pacific. However, this difference may arise from differences in the lower stratospheric circulation rather than from differences in vertical transport in the troposphere. Of course there have been many previous studies which highlight the strong differences between NH summer and NH winter, but it is important to keep in mind the precise measure of the circulation that is being considered. Fueglistaler et al. (2004, 2005) showed the low-level source region for air that subsequently reaches the stratosphere (and therefore determines stratospheric water vapour), but there was no particular criterion on transport timescale. Several studies have emphasised the role of the NH summer Asian monsoon anticyclone, with the relative isolation in the interior of the upper anticyclone leading to coherent features in water vapour (e.g. James et al., 2008) and in a variety of chemical species including CO, HCN, C_2H_6 and C_2H_2 (Park et al., 2008). Indeed Randel et al. (2010) have used HCN measurements to argue for a special role for the Asian monsoon anticyclone system in bringing polluted air from the south and east Asian region to the stratosphere in NH summer. However modelling studies such as Li et al. (2009) suggest that sources over a much broader geographical region are responsible for HCN variations. In any case HCN has a multi-year photochemical lifetime and an oceanic sink. Independent verification of the seasonal variations shown in Figs. 1 and 3 is more likely to come from observations of short-lived species such as Acetylene (C_2H_2), but the effects of seasonal variations in convective transport would have to be distinguished from seasonal variations in surface emissions.

The results presented here consider only the effect of trajectories that penetrate above 380 K. It has been noted (Levine et al., 2007) that there may be significant ozone depletion in the lowermost stratosphere due to VSLS and their product gases which are transported quasi-horizontally into the lowermost stratosphere. This could be included in our estimates by adopting a different definition of the control surface $\partial\Omega$. However, we note that residence times within the lower stratosphere are likely to be no more than a few months (compared with the 15 months for air transported across 380 K). Additionally, the results presented in Berthet et al. (2007) suggest that transport into the lowermost stratosphere in NH winter may be significantly less than that estimated by Levine et al. (2007).

Another potential sensitivity in our calculations is the assumption of a uniform decay rate λ for total halogen. As noted previously, this represents a combination of photochemical destruction of SG and loss of PGs through chemical degradation and washout. If removal of total halogen in the upper troposphere is overestimated through this assumption then ODPs might be larger than estimated here. Certainly transport timescales in the tropical upper troposphere appear to be relatively long, e.g., Krüger et al. (2009) estimate, on the basis of trajectory calculations similar to those used in this paper, that the time to ascend from 360 K to 380 K may be 30 d or more, though, as noted previously, deep convection over particular regions may penetrate high into the TTL (Fierli et al., 2010) thereby reducing transport timescales. In the case that air resides for 30 d or more in the TTL, our assumption of 20 d exponential decay would imply significant reduction in total halogen before reaching 380 K. The latter reduction in total halogen might well be an overestimate since, if convective penetration into this region is relatively rare, then removal by washout in this region is likely to be slow. On the other hand there is also the possibility of removal of total halogen through uptake on thin cirrus clouds which form as part of the process of dehydration of air as it enters the stratosphere (Sinnhuber and Folkins, 2006).

4 Conclusions

Calculating ODPs for VSLS is challenging because the ODPs are expected to be strong functions of location and time of emission, implying the need for many calculations with different emission distributions. Ultimately, multiple

calculations are needed with global 3-D models that represent both the tropospheric chemistry and transport processes that determine what fraction of the emitted halogen reaches the stratosphere, plus the stratospheric chemistry and transport processes that determine the resulting ozone depletion, but currently these are computationally expensive. Up to now ODP estimates have usually been based on simplified approaches that, for example, follow tropospheric evolution in some detail to predict the fraction of the halogen reaching the stratosphere, followed by some kind of approximate calculation of the implied ODP (e.g., Bridgeman et al., 2000; Olsen et al., 2000; Wuebbles et al., 2001). The exception is Wuebbles et al. (2009, 2010) which used a 3-D model of both troposphere and stratosphere.

Here, we have set out a trajectory-based methodology that gives the ODP as a function of location and time of emission. We believe the trajectory-based calculation to be as good a representation of tropospheric transport processes as an Eulerian CTM, not least because it is based on the same sort of velocity dataset that is typically used for an Eulerian calculation. The stratospheric calculation makes similar approximations to those that have been used before to estimate ODPs and indeed for long-lived species we see some advantage to our approach since it requires integration not for the lifetime of the emitted species but only for the time required to estimate the stratospheric residence time of the resulting active species. Furthermore, the separation of the calculation into tropospheric and stratospheric parts allows significant computational saving.

The calculations presented here are based on the simplest possible representation of tropospheric chemistry. Therefore, the primary interest in the results is not so much the absolute value of the ODPs but the implied spatial and temporal variation. The results shown in Fig. 4 show clearly that not only is there strong latitudinal variation, as has been suggested by previous work, but also that there is very significant longitudinal and seasonal variation. This is not unexpected from previous analysis of transport in the tropical troposphere, but our results are, we believe, the first quantitative estimates of implications for ODPs. The estimated ODPs are much higher than previous estimates in certain localised regions. (A recent paper by Brioude et al. (2010), submitted after this paper, includes a more detailed representation of tropospheric chemistry and suggests that our 20 day timescale for n-PB may be too long, implying that our estimated numerical values of ODPs should be smaller. But the strong dependence on location and season of the source is also found by Brioude et al. (2010), albeit in a less detailed analysis which does not include any analogue of our Fig. 4 showing ODP as a function of position.)

Extension to more sophisticated tropospheric or stratospheric chemistry would be possible without recalculation of the large trajectory dataset on which the estimates are based. Existing chemical trajectory codes could be used for both tropospheric and stratospheric parts of the calculation, with background chemical fields taken from a suitable Eulerian CTM. Representation of removal by moist processes would also be relatively straightforward to incorporate. The sensitivity demonstrated here of the estimated ODPs to the inclusion of convective parametrization emphasises the current quantitative uncertainty over precise values of ODPs. Even if it is accepted that a convective scheme is necessary the estimated values are likely to be depend on which particular convective scheme is chosen and any communication of ODPs to policymakers needs to emphasise the range of uncertainty associated with representation of convection or of any other processes.

Space and time integrals of the calculated ODP distributions, can be calculated straightforwardly to give overall ODPs for many different emissions scenarios. This would allow estimation of, for example, regional ODPs or ODPs for particular ship or aircraft routes. Detailed tables (large arrays) could be easily produced for automated evaluation for the use of policymakers.

Extension to different halogen-containing species (chlorinated, brominated, iodinated) would also be straightforward using different values of α or with a more sophisticated chemistry schemes. In particular, it would be possible to calculate ODPs for naturally occuring bromine species emitted by the tropical ocean (see e.g. Warwick et al., 2006) and to consider, for example, how the ODPs change as tropical ocean temperatures change in the future (e.g. considering the wind fields from a climate model). Correspondingly, ODPs for new artificial halogenated species could be estimated, given knowledge of their emissions, which might result from manufacture, use and disposal. NH midlatitudes have conventionally been seen as likely source regions for such species and ODPs would then be correspondingly small. But emissions resulting form continuing industrialisation and population growth in south and south-east Asia would clearly from Fig. 4 have a much larger potential impact on stratospheric ozone. This focuses attention on the precise spatial variation of the ODP distribution in this region and its relation to convecting regions. The pattern of low-level inflow into the Asian monsoon and its relation to potential emissions is a crucial aspect requiring further investigation.

Acknowledgements. This work was supported by the EU SCOUT-O3 Integrated Project (GOCE-CT-2004505390). We thank Gavin Esler, Stephan Fueglistaler, Sue Liu and Kirstin Krüger for useful discussions. Part of the calculations were performed using CICLAD, the computing system of IPSL.

Edited by: A. Baumgaertner

The publication of this article is financed by CNRS-INSU.

References

Aschmann, J., Sinnhuber, B.-M., Atlas, E. L., and Schauffler, S. M.: Modeling the transport of very short-lived substances into the tropical upper troposphere and lower stratosphere, Atmos. Chem. Phys., 9, 9237–9247, doi:10.5194/acp-9-9237-2009, 2009.

Berthet, G., Esler, J. G., and Haynes, P. H.: A Lagrangian perspective of the tropopause and the ventilation of the lowermost stratosphere, J. Geophys. Res., 112, D18102, doi:10.1029/2006JD008295, 2007.

Bridgeman, C. H., Pyle, J. A., and Shallcross, D. E.: A three-dimensional model calculation of the ozone depletion potential of 1-bromopropane (1-C3H7Br), J. Geophys. Res., 105, 26493–26502, 2000.

Brioude, J., Portmann, R. W., Daniel, J. S., Cooper, O. R., Frost, G. J., Rosenlof, K. H., Granier, C., Ravishankara, A. R., Montzka,S. A. and Stohl, A.: Variations in ozone depletion potentials of very short-lived substances with season and emission region. Geophys. Res. Lett., 37, L19804, doi:10.1029/2010GL044856, 2010.

Butler, J. H., King, D. B., Lobert, J. M., Montzka, S. A., Yvon-Lewis, S. A., Hall, B. D., Warwick, N. J., Mondeel, D. J., Aydin, M., and Elkins, J. W.: Oceanic distributions and emissions of short-lived halocarbons, Global Biogeochem. Cy., 21, GB1023, doi:10.1029/2006GB002732, 2007.

Dorf, M., Butz, A., Camy-Peyret, C., Chipperfield, M. P., Kritten, L., and Pfeilsticker, K.: Bromine in the tropical troposphere and stratosphere as derived from balloon-borne BrO observations, Atmos. Chem. Phys., 8, 7265–7271, doi:10.5194/acp-8-7265-2008, 2008.

Fierli, F., Orlandi, E., Law, K. S., Cagnazzo, C., Cairo, F., Schiller, C., Borrmann, S., Didonfrancesco, G., Ravegnani, F., and Volk, M.: Impact of deep convection in the tropical tropopause layer in West Africa: in-situ observations and mesoscale modelling, Atmos. Chem. Phys. Discuss., 10, 4927–4961, doi:10.5194/acpd-10-4927-2010, 2010.

Forster, C., Stohl, A., and Seibert, P.: Parameterization of convective transport in a Lagrangian particle dispersion model and its evaluation, J. Appl. Meteorol. Climatol., 46, 403–422, doi:10.1175/JAM2470.1, 2007.

Fueglistaler, S., Wernli, H., and Peter, T.: Tropical troposphere-to-stratosphere transport inferred from trajectory calculations, J. Geophys. Res., 109, D03108, doi:10.1029/2003JD004069, 2004.

Fueglistaler, S., Bonazzola, M., Haynes, P. H., and Peter, T.: Stratospheric water vapor predicted from the Lagrangian temperature history of air entering the stratosphere in the tropics, J. Geophys. Res., 110, D08107, doi:10.1029/2004JD005516, 2005.

Fueglistaler, S., Dessler, A. E., Dunkerton, T. J., Folkins, I., Fu, Q., and Mote, P. W.: Tropical tropopause layer, Rev. Geophys., 47, RG1004, doi:10.1029/2008RG000267, 2009.

Gettelman, A., Lauritzen, P. H., Park, M., and Kay, J. E.: Processes regulating short-lived species in the tropical tropopause layer, J. Geophys. Res., 114, D13303, doi:10.1029/2009JD011785, 2009.

Hack, J. J.: Parameterization of moist convection in the National Center for Atmospheric Research Community Climate Model (CCM2), J. Geophys. Res., 99, 5551–5568, 1994.

Hossaini, R., Chipperfield, M. P., Monge-Sanz, B. M., Richards, N. A. D., Atlas, E., and Blake, D. R.: Bromoform and dibromomethane in the tropics: a 3-D model study of chemistry and transport, Atmos. Chem. Phys., 10, 719–735, doi:10.5194/acp-10-719-2010, 2010.

James, R., Bonazzola, M., Legras, B., Surbled, K., and Fueglistaler, S.: Water vapor transport and dehydration above convective outflow during Asian monsoon, Geophys. Res. Lett., 35, L20810, doi:10.1029/2008GL035441, 2008.

Kerkweg, A., Jöckel, P., Pozzer, A., Tost, H., Sander, R., Schulz, M., Stier, P., Vignati, E., Wilson, J., and Lelieveld, J.: Consistent simulation of bromine chemistry from the marine boundary layer to the stratosphere – Part 1: Model description, sea salt aerosols and pH, Atmos. Chem. Phys., 8, 5899–5917, doi:10.5194/acp-8-5899-2008, 2008a.

Kerkweg, A., Jöckel, P., Warwick, N., Gebhardt, S., Brenninkmeijer, C. A. M., and Lelieveld, J.: Consistent simulation of bromine chemistry from the marine boundary layer to the stratosphere – Part 2: Bromocarbons, Atmos. Chem. Phys., 8, 5919–5939, doi:10.5194/acp-8-5919-2008, 2008b.

Krüger, K., Tegtmeier, S., and Rex, M.: Variability of residence time in the Tropical Tropopause Layer during Northern Hemisphere winter, Atmos. Chem. Phys., 9, 6717–6725, doi:10.5194/acp-9-6717-2009, 2009.

Law, K. S., Fierli, F., Cairo, F., Schlager, H., Borrmann, S., Streibel, M., Real, E., Kunkel, D., Schiller, C., Ravegnani, F., Ulanovsky, A., D'Amato, F., Viciani, S., and Volk, C. M.: Air mass origins influencing TTL chemical composition over West Africa during 2006 summer monsoon, Atmos. Chem. Phys., 10, 10753–10770, doi:10.5194/acp-10-10753-2010, 2010.

Legras, B., Joseph, B., and Lefèvre, F.: Vertical diffusivity in the lower stratosphere from Lagrangian back-trajectory reconstructions of ozone profiles, J. Geophys. Res., 108, 4562, doi:10.1029/2002JD003045, 2003.

Levine, J., Braesicke, P., Harris, N. R. P., Savage, N. H., and Pyle, J. A.: Pathways and timescales for troposphere to-stratosphere transport, J. Geophys. Res., 112, D04308, doi:10.1029/2005JD006940, 2007.

Li, Q., Palmer, P. I., Pumphrey, H. C., Bernath, P., and Mahieu, E.: What drives the observed variability of HCN in the troposphere and lower stratosphere?, Atmos. Chem. Phys., 9, 8531–8543, doi:10.5194/acp-9-8531-2009, 2009.

Olsen, S., Hannegan, B. J., Zhu, X., and Prather, M.: Evaluating ozone depletion from very short-lived halocarbons, Geophys. Res. Lett., 27, 1475–1478, 2000.

Park, M., Randel, W. J., Emmons, L. K., Bernath, P. F., Walker, K. A., and Boone, C. D.: Chemical isolation in the Asian monsoon anticyclone observed in Atmospheric Chemistry Experiment (ACE-FTS) data, Atmos. Chem. Phys., 8, 757–764, doi:10.5194/acp-8-757-2008, 2008.

Randel, W. J., Park, M., Emmons, L., Kinnison, D., Bernath, P., Walker, K. A., Boone, C., and Pumphrey, H.: Asian monsoon transport of pollution to the stratosphere, Science, 328, 611–613,

2010.

Salawitch, R. J., Weisenstein, D. K., Kovalenko, L. J., Sioris, C. E., Wennberg, P. O., Chance, K., Ko, M. K. W., and McLinden, C. A.: Sensitivity of ozone to bromine in the lower stratosphere, Geophys. Res. Lett., 32, L05811, doi:10.1029/2004GL021504, 2005.

Sinnhuber, B.-M. and Folkins, I.: Estimating the contribution of bromoform to stratospheric bromine and its relation to dehydration in the tropical tropopause layer, Atmos. Chem. Phys., 6, 4755–4761, doi:10.5194/acp-6-4755-2006, 2006.

Solomon, S. and Albritton, D. L.: Time dependent ozone depletion potentials for short- and long-term forecasts, Nature, 357, 33–37, 1992.

Solomon, S., Mills, M., Heidt, L. E., Pollock, W., and Tuck, A. F.: On the evaluation of ozone depletion potentials, J. Geophys. Res., 97, 824–842, 1992.

Stohl, A., Forster, C., Frank, A., Seibert, P., and Wotawa, G.: Technical note: The Lagrangian particle dispersion model FLEXPART version 6.2, Atmos. Chem. Phys., 5, 2461–2474, doi:10.5194/acp-5-2461-2005, 2005.

Tost, H., Lawrence, M. G., Brühl, C., Jöckel, P., The GABRIEL Team, and The SCOUT-O3-DARWIN/ACTIVE Team: Uncertainties in atmospheric chemistry modelling due to convection parameterisations and subsequent scavenging, Atmos. Chem. Phys., 10, 1931–1951, doi:10.5194/acp-10-1931-2010, 2010.

Warwick, N. J., Pyle, J. A., Carver, G. D., Yang, X., Savage, N. H., O'Connor, F. M., and Cox, R. A.: Global modeling of biogenic bromocarbons, J. Geophys. Res., 111, D24305, doi:10.1029/2006JD007264, 2006.

Waugh, D. W. and Hall, T. M.: Age of stratospheric air: theory, observations, and models, Rev. Geophys., 40(4), 1010, doi:10.1029/2000RG000101, 2002.

WMO: Scientific Assessment of Ozone Depletion: 2002, Tech. Rep. 47, World Meteorological Organization, Geneva, 2003.

WMO: Scientific Assessment of Ozone Depletion: 2006, Tech. Rep. 50, World Meteorological Organization, Geneva, 2007.

Wuebbles, D. J.: Chlorocarbon emission scenarios: potential impact on stratospheric ozone, J. Geophys. Res., 88, 1433–1443, 1983.

Wuebbles, D. J., Patten, K., Johnson, M., and Kotamarthi, R.: New methodology for ozone depletion potentials of short-lived compounds: n-propyl bromide as an example, J. Geophys. Res., 106, 14551–14571, 2001.

Wuebbles, D. J, Youm, D., Patten, K., and Avilés, M. M.: Metrics for Ozone and Climate: Three-Dimensional Modeling Studies of Ozone Depletion Potentials and Indirect Global Warming Potentials, in: Twenty Years of Ozone Decline, 297–326, doi:10.1007/978-90-481-2469-5_23, 2009.

Wuebbles, D. J., Patten, K. O., Wang, D., Youn, D., Martínez-Avilés, M., and Francisco, J. S.: Three-dimensional model evaluation of the Ozone Depletion Potentials for n-propyl bromide, trichloroethylene and perchloroethylene, Atmos. Chem. Phys. Discuss., 10, 17889–17910, doi:10.5194/acpd-10-17889-2010, 2010.

Zhang, G. J. and McFarlane, N. A.: Sensitivity of climate simulations to the parameterization of cumulus convection in the Canadian Climate Centre general circulation model, Atmos.-Ocean, 33, 407–446, 1995.